

# Coupled Effects of Energy Dissipation and Travelling Velocity in the Run-Out Simulation of High-Speed Granular Masses

Francesco Federico<sup>1</sup>, Giuseppe Favata

<sup>1</sup>*University of Rome "Tor Vergata", Rome, Italy*

*E-mail: fdrfnc@gmail.com*

*Received February 1, 2011; revised April 5, 2011; accepted June 2, 2011*

## Abstract

The run-out of high speed granular masses or avalanches along mountain streams, till their arrest, is analytically modeled. The power balance of a sliding granular mass along two planar sliding surfaces is written by taking into account the mass volume, the slopes of the surfaces, the fluid pressure and the energy dissipation. Dissipation is due to collisions and displacements, both localized within a layer at the base of the mass. The run-out, the transition from the first to the second sliding surface and the final run-up of the mass are described by Ordinary Differential Equations (ODEs), solved in closed form (particular cases) or by means of numerical procedures (general case). The proposed solutions allow to predict the run-up length and the speed evolution of the sliding mass as a function of the involved geometrical, physical and mechanical parameters as well as of the simplified rheological laws assumed to express the energy dissipation effects. The corresponding solutions obtained according to the Mohr-Coulomb or Voellmy resistance laws onto the sliding surfaces are recovered as particular cases. The run-out length of a documented case is finally back analysed through the proposed model.

**Keywords:** Sliding Granular Mass, Granular Temperature, Shear Layer, Excess Interstitial Pressure

## 1. Introduction

Great attention receives in scientific community the study of kinematic mechanisms of the flow of viscous fluid [1] or the chaotic movement of granular masses [2], because their destroying effects, often related to increasing anthropization of piedmont areas. It is necessary to identify hazardous areas for the propagation of high-speed moving masses. To this purpose, reliable criteria must be formulated and applied.

Interstitial pressures at the base of the mass can vary from null or hydrostatic value to high values, due to possible water pressure excess, related to very rapid changes of pore volumes, often localized along a thin layer in proximity of the sliding surface [3].

Several models assume the validity of the Mohr-Coulomb (M-C) shear resistance criterion [4] along the sliding surface of the high-rate moving mass. To match experimental observations of the run-out length with theoretical results, small shear resistance angles must be assumed. The M-C law usually describes limit equi-

librium (static) or simple sliding of *blocks* along rough surfaces (dynamic condition). More complex resistance laws should be taken into account [5] to describe the rapid sliding of *granular masses* because high speed relative motion and collisions between solid grains take place within a basal shear layer, causing a *fluidification* effect coupled with energy dissipations [6]. Therefore, it is not conceptually justifiable the reduction of the shear resistance angle, due to the high mobility of the grains [7] if the corresponding energy dissipation is not taken into account. Moreover, in situ observations show that the run-out length strongly depends on the mobilized volume of the mass [8-11].

In the paper, the rapid sliding of a granular mass along two planar surfaces is analytically modelled by accounting for the effects of grain collisions.

In section 2 the main features of the model and the assumed simplifying hypotheses are introduced; the governing equations are formulated (section 3), by introducing the parameters which take into account the *granular temperature* and the collisional dissipated energy.

Closed form or numerical solutions of the ODEs are then obtained (section 4). After an estimate of the model parameters, in section 5 some parametric results of run-out length are represented and compared to solutions obtained according to the M-C or Voellmy (V) resistance criteria along the base of the sliding mass. The schematic back analysis of a case is carried out through the model in section 6. Some concluding remarks close the paper.

## 2. Analytical Model

### 2.1. Basic Assumptions

Three phases roughly characterize rapid landslides motion, after their detachment (avalanches) or trigger (debris flow): 1) the mass runs along the first sliding surface (s.s.) (run-out), 2) the initial portion of the mass slides along the counterslope s.s. while the remaining portion still moves along the first one, 3) the whole mass runs up along the counterslope s.s., till its stop (**Figure 1**). Moreover:

- Planar sliding surfaces are assumed (**Figure 1**): the slope angles of the first and second s.s. are  $\theta > 0$  and  $\alpha \leq 0$ , respectively. The run-out length along the first surface is  $L$ ;

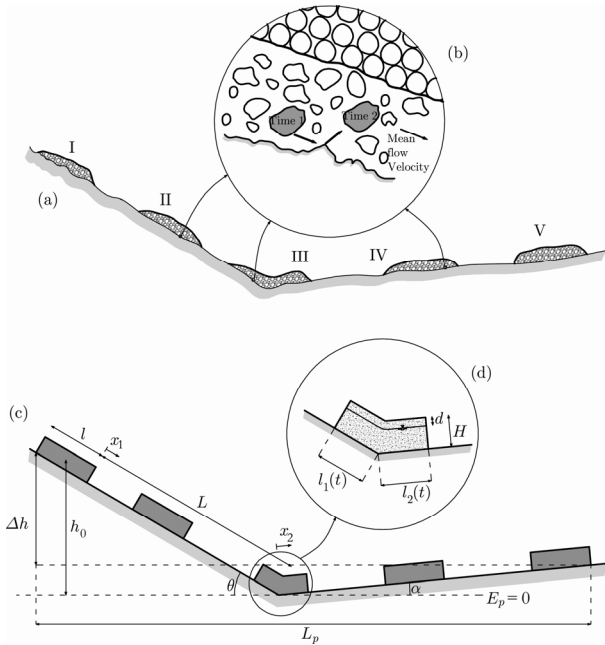


**Figure 1.** (a) Phases of rapid landslides or avalanches motion: I - detachment and initial conditions; II - run-out; III - transition of the moving mass from the first to the second inclined planar surface; IV - run-up; V - final position; (b) shear layer in proximity of the basal sliding surface; fluctuations of particles velocity around their average value, occur; (c) problem setting for computations; (d) transition from the first to the second sliding plane.

- the sliding granular mass is schematized as a parallelepiped (length  $l$ , height  $H$  and depth  $D$ ) whose geometry doesn't vary; erosion or deposition processes are not considered;
- a "shear layer" at the base of the mass takes place during the rapid sliding. This small thickened layer (compared to  $H$ ) is composed by particles that move at high velocity and collide each with others. Collisions induce appreciable fluctuations of their velocities (granular temperature);
- the energy dissipation due to the mass straining coupled with the mass displacements, is neglected.

### 2.2. Governing Equations

The power balance of the sliding mass holds:

$$\frac{dE_p}{dt} + \frac{dE_c}{dt} + \frac{dE_{na1}}{dt} + \frac{dE_{na2}}{dt} = 0 \quad (1)$$

$E_p$  being the potential energy,  $E_c$  the kinetic energy of the sliding mass. The dissipated energy ( $E_{na}$ ), not more available for the motion, is schematically splitted in two components:  $E_{na1}$ , lost due to the (Coulomb's) friction along the sliding surface;  $E_{na2}$ , transferred from the block to the basal "shear layer" [2,7,12]. The (1) is in the following rewritten for each phase of the motion.

### 2.3. Transfer and Dissipation of Energy

$E_{na1}$  is a function of the weight  $W$  of the sliding mass, the resultant  $U$  of the interstitial fluid pressures, the shear resistance angle  $\phi_b$  at the base of the block, reduced with respect to the shear resistance angle  $\phi'$  of the involved material, due to the peculiar physical conditions (high speed, collisions) along the s.s., the path  $x$ .

The energy  $E_{na2}$  transferred to the "shear layer" [2,7, 12], is lost by the granular mass during its running along the first s.s.;  $E_{na2}$  may be partially recovered by the mass and correspondingly lost by the "shear layer", along the run-up (counterslope). The analytical expression of  $E_{na2}$  is not *a priori* known: it is hypothesized its dependence upon the rate  $v$  of the granular mass. As stated by [6], the maximum value of the function  $dE_{na2}/dt$  is obtained if the rate  $v = \dot{x}_1(t)$  attains a constant value, whatever be its value. Therefore,  $dE_{na2}/dt$  has been defined as follows:

$$\frac{dE_{na2}}{dt} = \chi_\theta(v) \left( \frac{dE_{na2}}{dt} \right)_{\max} \quad (2)$$

the adimensional function  $0 \leq \chi_\theta(v) \leq 1$  depending on  $v$ . If  $\chi_\theta(v) = 0$ , the energy is not transferred from the mass to the shear layer (granular temperature) or *vice-versa*; the limit case  $\chi_\theta(v) = 1$  implies that the energy transfer is maximized, being  $v = \text{const}$ .

### 2.4. Effects of Interstitial Pressures

The interstitial pressure  $p_w(x)$  at the base of the mass affects the run-out length;  $p_w(x)$  simply assumes the constant value  $p_w$  (nil value as limit case) through the relation:  $p_w = \gamma_w(H - d)$  (Figure 1),  $\gamma_w$  being the specific weight of the water;  $d = 0$  if the whole mass is saturated;  $d = H$  if the mass is dry;  $p_w$  may exceed the hydrostatic value due to the mechanical effects associated with the rapid change of intergranular volumes of the voids and the corresponding growth of interstitial water pressures excess [3,6]. To simulate this effect,  $d < 0$  values must be assigned. The length  $d$  thus lies in the range:

$$d_{\min} \leq d \leq d_{\max} = H \tag{3}$$

If the sliding granular mass always transmits positive normal stresses to the s.s., through the shear layer, the minimum value  $d_{\min}$  can be deduced by imposing the equilibrium along the direction orthogonal to the sliding plane:

$$-d_{\min} = \min \left\{ \left( \frac{\gamma_t}{\gamma_w} \cos \theta - 1 \right) H; \left( \frac{\gamma_t}{\gamma_w} \cos \alpha - 1 \right) H \right\} \tag{4}$$

$\gamma_t$  being the unit weight of the sliding mass and  $d_{\min}$  a negative real number.

### 2.5. Sliding along the First Slope

The potential energy  $E_p$  in the power balance (1) is rewritten in function of the abscissa  $x_1$  (Figure 1) as follows:

$$E_p = mg(h_0 - x_1 \sin \theta) \tag{5}$$

$h_0$  being the initial elevation of the centre of mass with respect to a reference plane;  $g$  the gravity acceleration and  $m$  the mass of the sliding granular body.

The dissipated energy  $E_{na1}(x_1)$  is then rewritten as follows:

$$E_{na1}(x_1) = \int_0^{x_1} (W \cos \theta - U) \tan \phi_b ds \tag{6}$$

$$= (W \cos \theta - U) \tan \phi_b x_1$$

$U < W \cos \theta$  being the global force associated with the pressure  $p_w$  at the base of the mass,  $W$  the mass weight and  $\phi_b$  the reduced shear resistance angle at the base of the mass.

The dissipated energy  $E_{na2}$  (2) depends upon the rate  $v$  of the granular mass.

According to (5), (6), the equation (1) is rewritten as:

$$mg \sin \theta \dot{x}_1(t) = \frac{1}{2} m \frac{d\dot{x}_1^2(t)}{dt} \tag{7}$$

$$+ (W \cos \theta - U) \tan \phi_b \dot{x}_1(t) + \frac{dE_{na2}}{dt}$$

The maximum value for  $dE_{na2}/dt$  is gained if  $v = \dot{x}_1(t)$  assumes a constant value [6]. It may be written:

$$\frac{dE_{na2}}{dt} \Big|_{\max} = [W \sin \theta - (W \cos \theta - U) \tan \phi_b] \dot{x}_1(t) \tag{8}$$

Recalling the (2),  $dE_{na2}/dt$  becomes:

$$\frac{dE_{na2}}{dt} = \chi_\theta(v) [W \sin \theta - (W \cos \theta - U) \tan \phi_b] \dot{x}_1(t) \tag{9}$$

the function  $0 \leq \chi_\theta(v) \leq 1$  being previously introduced.

By replacing the (9) in (7), it is obtained:

$$\frac{1}{2} \frac{d(\dot{x}_1^2(t))}{dt} \tag{10}$$

$$= g \left[ \sin \theta - \left( \cos \theta - \frac{U}{W} \right) \tan \phi_b \right] [1 - \chi_\theta(v)] \dot{x}_1(t)$$

The ratio  $U/W$  is rewritten as:

$$\frac{U}{W} = \frac{\gamma_w(H - d)lD}{\gamma_t H l D} = \frac{\gamma_w}{\gamma_t} \left( 1 - \frac{d}{H} \right) \tag{11}$$

So, the Equation (11) becomes:

$$\frac{1}{2} \frac{d(\dot{x}_1^2(t))}{dt} \tag{12}$$

$$= g \left[ \tan \theta - \tan \phi_b + \frac{\gamma_w \tan \phi_b}{\gamma_t \cos \theta} \left( 1 - \frac{d}{H} \right) \right] [1 - \chi_\theta(v)] \dot{x}_1(t)$$

Let be

$$R_\theta = R_\theta(\theta, d, H) = 1 - \frac{\gamma_w}{\gamma_t \cos \theta} \left( 1 - \frac{d}{H} \right) \tag{13}$$

The derivative of equation (12) gets:

$$\ddot{x}_1(t) = g \cos \theta (\tan \theta - R_\theta \tan \phi_b) [1 - \chi_\theta(v)] \tag{14}$$

According to the assumed hypotheses, the time derivative of the energy component  $E_{na2}$ , for unit mass, is:

$$\frac{dE_{na2}}{dt} = g \cos \theta (\tan \theta - R_\theta \tan \phi_b) \chi_\theta(v) \tag{15}$$

Through the (15), the discriminant value  $\theta^*$  for which  $dE_{na2}/dt = 0$  may be determined, by solving the equation:

$$g \cos \theta^* (\tan \theta^* - R_\theta \tan \phi_b) \chi_{\theta^*}(v) = 0 \tag{16}$$

If the slope angle  $\theta < \theta^*$ ,  $dE_{na2}/dt < 0$ : the sliding mass receives energy from the shear layer. If  $\theta > \theta^*$ ,  $dE_{na2}/dt > 0$ : the sliding mass provides energy to the shear layer.

Being interesting only the conditions  $\cos \theta^* > 0$  and  $\chi_{\theta^*}(v) > 0$ , according to the (13), the (16) becomes:

$$\tan \theta^* - \left[ 1 - \frac{\psi}{\cos \theta^*} \right] \tan \phi_b = 0 \quad (17)$$

Through the (17),  $\theta^*$  is obtained:

$$\theta^* = \arccos \left[ \cot \phi_b \left( \psi \tan \phi_b - \frac{\psi \tan \phi_b}{1 + (\tan \phi_b)^2} + \frac{\sqrt{(\tan \phi_b)^2 + (\tan \phi_b)^4 - \psi^2 (\tan \phi_b)^4}}{1 + (\tan \phi_b)^2} \right) \right] \quad (18)$$

$$\psi = (\gamma_w / \gamma_t)(1 - d/H) \quad (19)$$

In the simple case  $d = H$  (no interstitial fluid pressure), it results  $\psi = 0$  and the equation (18) gets  $\theta^* = \phi_b$ .

The sign of the derivative  $dE_{na2}/dt$  depends on the sign of the expression  $(\tan \theta - R_\theta \tan \phi_b)$ , the other terms being positive. This sign is positive along the first planar s.s. (otherwise, the motion cannot take place), while is negative along the second s.s., because we must replace  $\theta > 0$  with  $\theta < \theta^*$  (reduced slope) or  $\alpha \leq 0$  (counterslope).

### 2.6. Sliding along the Counterslope Surface

The motion law along the counterslope s.s. is obtained by substituting in the (14) the angle  $\theta > 0$  with  $\alpha \leq 0$ ; correspondingly, the function  $\chi_\theta(v)$  must be replaced by  $\chi_\alpha(v)$ :

$$\ddot{x}_2(t) = g \cos \alpha (\tan \alpha - R_\alpha \tan \phi_b) [1 - \chi_\alpha(v)] \quad (20)$$

where:

$$R_\alpha = 1 - \frac{\gamma_w}{\gamma_t \cos \alpha} \left( 1 - \frac{d}{H} \right) \quad (21)$$

The ODE (20) must be solved taking into account the following initial conditions:

$$x_2(0) = 0; \quad \dot{x}_2(0) = v_0$$

$v_0$  being the velocity of the mass after the full transition from the first to the second sliding planar surface.

### 2.7. Transition from the First to the Second Slope

By neglecting the additional lost of energy coupled with peculiar strains associated with the slope change of the s.s., the ODE expressing the motion during the transition phase may be approximated through the linear combination of (14) and (20):

$$\left\{ \ddot{x}_{12}(t) - g \cos \theta (\tan \theta - R_\theta \tan \phi_b) [1 - \chi_\theta(v)] \right\} l_1(t) + \left\{ \ddot{x}_{12}(t) - g \cos \alpha (\tan \alpha - R_\alpha \tan \phi_b) [1 - \chi_\alpha(v)] \right\} l_2(t) = 0 \quad (22)$$

$l_1(t)$  being the length of the portion of the granular mass resting on the first surface and  $l_2(t) = x_{12}(t)$  the length of the remaining part running up along the second plane (run-up). So,  $l_1(t) + l_2(t) = l$ , neglecting second order geometrical aspects and accounting for the considerable length of the sliding granular mass (**Figure 1(d)**).

After some algebra, Equation (22) can be written as:

$$\ddot{x}_{12}(t) = \frac{g}{l} \cos \theta (\tan \theta - R_\theta \tan \phi_b) [1 - \chi_\theta(v)] [l - x_{12}(t)] + \frac{g}{l} \cos \alpha (\tan \alpha - R_\alpha \tan \phi_b) [1 - \chi_\alpha(v)] x_{12}(t) \quad (23)$$

The second term figuring in the expressions  $R_\theta$  and  $R_\alpha$  represents the contribution due to interstitial pressures; it is always positive because  $d \leq H$ . By decreasing  $d$  (the free surface moves towards the top of the mass)  $R_\theta$  and  $R_\alpha$  decrease; the terms  $(\tan \theta - R_\theta \tan \phi_b)$  and  $(\tan \alpha - R_\alpha \tan \phi_b)$  consequently increase. So, all other factors assuming constant values, the acceleration will be as greater as smaller is  $d$ .

### 2.8. Acceleration and limit rate

Referring to the acceleration along each sliding surface, equations (14) and (20) can be rewritten as follows:

$$\ddot{x}(t) = g \cos \zeta (\tan \zeta - R_\zeta \tan \phi_b) [1 - \chi_\zeta(v)] \quad (24)$$

where:

$$R_\zeta = 1 - \frac{\gamma_w}{\gamma_t \cos \zeta} \left( 1 - \frac{d}{H} \right) \quad (25)$$

$$\zeta = \begin{cases} \theta > 0 & \text{for } 0 \leq x \leq L \\ \alpha \leq 0 & \text{for } x \geq L + l \end{cases} \quad (26)$$

The term  $r(v) = g \cos \zeta [1 - \chi_\zeta(v)]$  is always positive along both sliding surfaces ( $0 \leq \chi_\zeta(v) \leq 1$ ). If the increase of the function  $\chi_\zeta(v)$  with the rate  $v$  of the mass is assumed, the function  $r(v)$  will decrease if  $v$  increases. Equation (24) can be thus rewritten as:

$$\ddot{x}(t) = r(v) (\tan \zeta - R_\zeta \tan \phi_b) \quad (27)$$

Coefficient  $R_\zeta \leq 1$  is equal to one if the interstitial pressures are equal to zero. Along the first surface,  $\tan \zeta - R_\zeta \tan \phi_b > 0$ , otherwise, the initial conditions  $x_1(0) = 0, \dot{x}_1(0) = 0$  would not allow the motion beginning; thus, the acceleration will be positive, the sliding rate will increase,  $r(v)$  will decrease and, consequently, a decrease of acceleration, always positive, will occur along the path. The acceleration will vanish if the rate approaches its limit value, for which  $r(v_{lim}) \rightarrow 0$ , or  $\chi_\zeta(v_{lim}) \rightarrow 1$ .

Along the second inclined plane,  $\tan \zeta - R_\zeta \tan \phi_b < 0$ : therefore, the acceleration now assumes negative values, the sliding rate will decrease,  $r(v)$  will increase and, consequently, the absolute value of acceleration (which is, however, negative) will increase.

### 3. Mathematical Model

#### 3.1. The $\chi(v)$ Function

The function  $\chi_\zeta(v)$  governs both transfer and dissipation of energy taking place near the sliding surfaces, due to multiple collisions between particles, as well as rotations of each particle around an axis [6]. The function  $\chi_\zeta(v) \in [0,1]$  has been analytically represented through a second order, rate increasing polynomial function:

$$\chi_\zeta(v) = \chi_0 + \lambda_\zeta v + \mu_\zeta v^2 \tag{28}$$

$\chi_0$  being an adimensional constant;  $\lambda_\zeta$  and  $\mu_\zeta$  are constants whose dimensions are the inverse of velocity and the inverse of square velocity, respectively ( $\zeta = \theta$  or  $\alpha$ ).

If  $\chi_\theta(v_{lim}) \rightarrow 1$ , it is obtained  $\ddot{x}_1(t) \rightarrow 0$ . The limit value of the rate corresponding to  $\ddot{x}_1(t) = 0$  of the sliding mass may be obtained by imposing:

$$\chi_0 + \lambda_\theta v_{lim} + \mu_\theta v_{lim}^2 = 1 \tag{29}$$

The (29) gets:

$$v_{lim} = \frac{-\lambda_\theta \pm \sqrt{\lambda_\theta^2 + 4\mu_\theta(1-\chi_0)}}{2\mu_\theta} \tag{30}$$

The negative solution of (30) is not significant.

Coefficients  $\chi_0$ ,  $\lambda_\zeta$  and  $\mu_\zeta$  cannot assume arbitrary values; they must respect the conditions deriving from the inequalities as well as from the definition domains of the integration constants (see sections 3.3 and 3.4), reported in **Table 1**.

#### 3.2. Equations of Motion

After substitution of (28) in (14), (20) and (22), the equations of motion, are written as follows:

**Table 1. Imposed conditions on the coefficients of the model,  $\chi_\zeta(v)$  being expressed by (28).**

Condition
$\mu_\zeta \neq 0$
$\lambda_\zeta^2 + 4\mu_\zeta(1-\chi_0) > 0$
$\frac{ 2v_0\mu_\alpha + \lambda_\alpha }{\sqrt{\lambda_\alpha^2 + 4\mu_\alpha(1-\chi_0)}} < 1$

$$\ddot{x}_1(t) - A + B\dot{x}_1(t) + Cx_1^2(t) = 0 \tag{31}$$

$$\ddot{x}_2(t) - D + E\dot{x}_2(t) + Fx_2^2(t) = 0 \tag{32}$$

$$\begin{aligned} &\ddot{x}_{12}(t) - A + B\dot{x}_{12}(t) + Cx_{12}(t) + \frac{A}{l}x_{12}(t) \\ &- \frac{B}{l}x_{12}(t)\dot{x}_{12}(t) - \frac{C}{l}x_{12}(t)x_{12}^2 + \frac{D}{l}x_{12}(t) \\ &+ \frac{E}{l}x_{12}(t)\dot{x}_{12}(t) + \frac{F}{l}x_{12}(t)x_{12}^2(t) = 0 \end{aligned} \tag{33}$$

where

$$A = g \cos \theta (\tan \theta - R_\theta \tan \phi_b) (1 - \chi_0) \tag{34a}$$

$$B = \lambda_\theta g \cos \theta (\tan \theta - R_\theta \tan \phi_b) \tag{34b}$$

$$C = \mu_\theta g \cos \theta (\tan \theta - R_\theta \tan \phi_b) \tag{34c}$$

$$D = g \cos \alpha (\tan \alpha - R_\alpha \tan \phi_b) (1 - \chi_0) \tag{34d}$$

$$E = \lambda_\alpha g \cos \alpha (\tan \alpha - R_\alpha \tan \phi_b) \tag{34e}$$

$$F = \mu_\alpha g \cos \alpha (\tan \alpha - R_\alpha \tan \phi_b) \tag{34f}$$

#### 3.3. Analytical Solution: Sliding along the First Slope

The integration of Equation (31) gets:

$$\begin{aligned} \dot{x}_1(t) = \frac{1}{2C^2} \left\{ -BC - C\sqrt{B^2 + 4AC} \cdot \right. \\ \left. \cdot \tanh \left[ \frac{\sqrt{B^2 + 4AC} (C_1 - Ct)}{2C} \right] \right\} \end{aligned} \tag{35}$$

$$\begin{aligned} x_1(t) = \frac{1}{2C^2} \left\{ B(C_1 - Ct) - 2C^2C_2 + \right. \\ \left. + 2C \ln \left[ \cosh \left( \frac{\sqrt{B^2 + 4AC} (C_1 - Ct)}{2C} \right) \right] \right\} \end{aligned} \tag{36}$$

The unknown constants  $C_1$  and  $C_2$  are determined through the initial conditions:

$$x_1(0) = 0, \quad \dot{x}_1(0) = 0$$

$$C_1 = \frac{2C}{\sqrt{B^2 + 4AC}} \operatorname{arctanh} \left( -\frac{B}{\sqrt{B^2 + 4AC}} \right) \tag{37a}$$

$$\begin{aligned} C_2 = \frac{B}{C\sqrt{B^2 + 4AC}} \operatorname{arctanh} \left( \frac{B}{\sqrt{B^2 + 4AC}} \right) \\ - \frac{1}{C} \ln \left( \frac{1}{2} \sqrt{\frac{B^2 + 4AC}{AC}} \right) \end{aligned} \tag{37b}$$

#### 3.4. Analytical Solution: Sliding along the Second Slope

The analytical integration of (32) (counterslope) gets:

$$\dot{x}_2(t) = \frac{1}{2F^2} \left\{ -EF - F\sqrt{E^2 + 4DF} \cdot \tanh \left[ \frac{\sqrt{E^2 + 4DF} (C_3 - Ft)}{2F} \right] \right\} \quad (38)$$

$$x_2(t) = \frac{1}{2F^2} \left\{ E(C_3 - Ft) + 2F^2 C_4 + 2F \ln \left[ \cosh \left( \frac{\sqrt{E^2 + 4DF} (C_3 - Ft)}{2F} \right) \right] \right\} \quad (39)$$

By imposing the conditions:

$$x_2(0) = 0, \quad \dot{x}_2(0) = v_0$$

the unknown constants are determined:

$$C_3 = \frac{2F}{\sqrt{E^2 + 4DF}} \operatorname{arctanh} \left( -\frac{2Fv_0 + E}{\sqrt{E^2 + 4DF}} \right) \quad (40a)$$

$$C_4 = \frac{E}{F\sqrt{E^2 + 4DF}} \operatorname{arctanh} \left( \frac{2Fv_0 + E}{\sqrt{E^2 + 4DF}} \right) - \frac{1}{F} \ln \left( \frac{1}{2} \sqrt{\frac{E^2 + 4DF}{E^2 + 4DF - (2Fv_0 + E)^2}} \right) \quad (40b)$$

### 3.5. Transition from the First to the Second Slope

The integration of (33) is carried out by means of a numerical procedure, by assigning initial conditions:

$$x_{12}(0) = 0, \quad \dot{x}_{12}(0) = v_{1f}$$

$v_{1f}$  being the rate of the sliding granular mass at the end of the first inclined planar s.s. To this aim, the fourth order Runge-Kutta method with adaptive step size has been implemented in MathCad.

It is worth observing that the proposed analytical solutions have been found referring to the trinomial formula  $\chi_\zeta(v)$  (28). If  $\chi_\zeta(v)$  is simply expressed by assuming  $\lambda_\zeta(v) = 0$  or  $\mu_\zeta(v) = 0$  or both, it is possible to express the analytical solution in closed form, also for the transition from the first towards the second s.s.

## 4. Characterization of the $\chi(v)$ function

### 4.1. Premise

The limits of the function  $\chi_\alpha(v)$  (Equation (20)) are the same as those assumed for the function  $\chi_\theta(v)$ . Part of the energy is given back to the sliding mass by the shear layer, whose granular temperature gradually decreases, due to the corresponding decrease of the average run-up

rate. If the inequalities  $0 \leq \chi_\alpha(v) \leq 1$  are taken into account, the maximum negative variation of lost energy, as well as the maximum variation of energy recovered by the sliding granular mass, cannot exceed the maximum value corresponding to the limit case  $v = \text{cost}$ . The time variation of energy lost due to granular temperature then assumes negative values along the second sliding surface; thus, the granular mass recovers energy by the shear layer. The function  $\chi_\theta(v)$  modulates the part of energy unavailable for the motion; it incorporates the effects due to granular temperature and collisional dissipations along the first inclined plane;  $\chi_\alpha(v)$ , the part of energy given back to the sliding granular mass, *net collisional dissipations*; then,  $\chi_\alpha(v)$  cannot be equal to  $\chi_\theta(v)$ : the inequality  $\chi_\alpha(v) < \chi_\theta(v)$  must always hold.

### 4.2. Coefficients

To estimate the parameters  $\chi_0$ ,  $\lambda_\zeta$ ,  $\mu_\zeta$  (function  $\chi_\zeta(v)$ ), it is first analyzed the simpler case  $\lambda_\zeta = 0$ .  $\lambda_\zeta$  is linearly related to the sliding rate and it is roughly correlated to the macro-viscous regime [14,15] that takes place only for small velocities of the granular mass; for a long and rapid sliding path, it does not seem prevalent.

Attention is so focused to  $\mu_\zeta$ , by assuming that  $\chi_0$  assumes the same value along both the sliding surfaces.

$\mu_\zeta$  cannot assume the same value along the two s.s. Along the first surface ( $\zeta = \theta$ ),  $\mu_\theta$  modulates the power subtracted to the granular mass, not available for the motion. A part, here defined  $\bar{\mu}$ , is stored as power related to granular temperature; the remaining part,  $\delta$ , is lost due to the collisions associated to the granular temperature. Therefore,  $\mu_\theta$  analytically expresses the sum of the powers related both to the granular temperature and collisional dissipation:

$$\mu_\theta = \bar{\mu} + \delta = \bar{\mu} \left( 1 + \frac{\delta}{\bar{\mu}} \right) \quad (41)$$

Along the counterslope plane ( $\zeta = \alpha$ ), the “stored” power  $\bar{\mu}$  is partly given back to the sliding mass ( $\mu_\alpha$ ) and partly dissipated through collisions. Therefore,  $\mu_\alpha$  represents the power given back to the granular mass; it must express the difference between the power previously “stored” ( $\bar{\mu}$ ) and the power again dissipated ( $\delta$ ):

$$\mu_\alpha = \bar{\mu} - \delta = \bar{\mu} \left( 1 - \frac{\delta}{\bar{\mu}} \right) \quad (42)$$

$\delta/\bar{\mu}$  represents the ratio between the powers ( $E_{coll}$ ) lost due to collisions and ( $E_{gt}$ ) stored through the granular temperature:

$$\frac{\delta}{\bar{\mu}} = k = \frac{\dot{E}_{coll}}{\dot{E}_{gt}} \quad (43)$$

To better express the ratio  $\delta/\bar{\mu}$ , the additional hypotheses of binary collisions and constant average mass  $m_g$  of the grains composing the sliding mass are assumed. It is possible to express  $E_{coll}$  as [13]:

$$E_{coll} = \frac{1}{4} m_g N_c (1 - e^2) \Delta v^2 \quad (44)$$

$\Delta v$  is the relative velocity between two colliding grains,  $e$  is their restitution coefficient, falling in the range 0 - 1, and  $N_c$  is the number of collisions.

The energy related to the granular temperature can be expressed, in turn, as [12]:

$$E_{gt} = \frac{1}{2} m_g N \delta v^2 \quad (45)$$

$N$ , number of grains,  $\delta v$ , average value of the modulus of the velocity fluctuation vector. If all grains collide,  $N_c = N/2$ ;  $\delta v$  and the relative velocity  $\Delta v$  may be related each other through the relation:

$$\Delta v = \beta \delta v \quad (46)$$

being  $0 < \beta \leq 2$ ; if  $\beta = 0$ , the relative velocities of all grains are null: therefore, no collisions take place. On the contrary,  $\beta = 2$  means that, for each collision, the two colliding grains, moving along the same direction, assume opposite velocity vectors; their relative velocity doubles the absolute velocity of each grain.

By further assuming  $\dot{N} = \dot{N}_c = 0$ , (43) becomes:

$$k = \frac{1}{4} (1 - e^2) \beta^2 \quad (47)$$

parameter  $k \in [0,1]$  (Figure 2).

Therefore, it is obtained:

$$\mu_\zeta = \bar{\mu} (1 \pm k) \quad (48)$$

the positive sign must be assumed if  $\zeta = \theta$ , while the negative one if  $\zeta = \alpha$ . The ratio  $r_\mu \geq 1$  is finally defined:

$$r_\mu = \frac{\mu_\theta}{\mu_\alpha} = \frac{1+k}{1-k} \quad (49)$$

If energy dissipation after collisions does not take place ( $k = 0$ ), along the whole path, it results  $r_\mu = 1$ .

To estimate parameters  $\chi_0$ ,  $\mu_\zeta$ , it may be observed that, if  $\lambda_\zeta = 0$ , the limit rate along the first s.s. is:

$$v_{lim} = \sqrt{\frac{1 - \chi_0}{\mu_\theta}} \quad (50)$$

Let us consider the high speed granular mass characterized by typical maximum velocities 20 - 40 m/s; a preliminary range for parameters  $\chi_0$ ,  $\bar{\mu}$  corresponding to these values of limit velocity is below obtained (Figure 3 and 4):  $\bar{\mu} = 5 \cdot 10^{-4} \div 10^{-3}$ ,  $\chi_0 = 0.2 \div 0.4$ .

The mobilized friction angle  $\phi_{mob}$  can be estimated

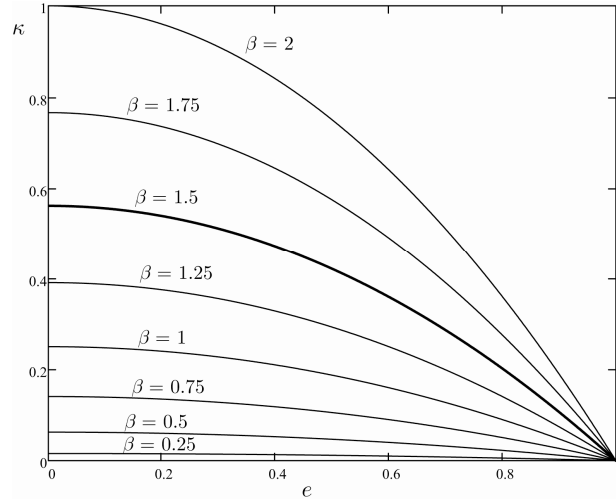


Figure 2. Parameter  $k$  vs. coefficient  $e$ , for some values of  $\beta$ .

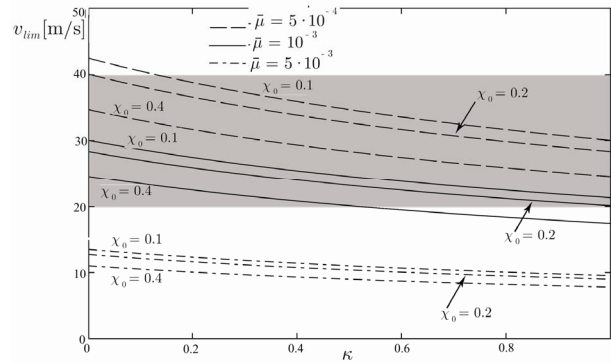


Figure 3. Couples  $\chi_0 - \bar{\mu}$  values, vs.  $k$ ;  $v_{lim} \in [20,40]$  m/s.

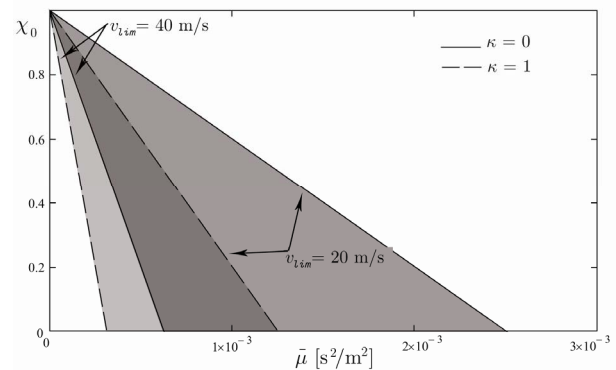


Figure 4. Range of admissible values for  $\chi_0$  and  $\bar{\mu}$ ;  $k=0$  or  $k=1$ ;  $20 \leq v_{lim} \leq 40$ .

through the empirical criteria, which express, as a function of the mobilized volume  $V$ , the ratio  $f(V) = \Delta h/L_p$ .

Through an empirical relationship, for a given sliding volume, it is possible to find the ratio  $f(V)$  and the total sliding length path  $L_T$ . Being the problem geometry known, the values of  $L$  (run-out length along the first

sliding surface),  $\theta$  (corresponding slope angle),  $x_{2f}$  the run-up length along the counterslope surface,  $l$  (length of the mass),  $L_T$  will depend upon  $\alpha$ , as follows:

$$L_T = L + l + x_{2f} = L + \frac{(L+l)(\sin \theta - f \cos \theta)}{f \cos \alpha - \sin \alpha} \quad (51)$$

By this way, at the base of the sliding granular mass, simultaneously frictional and collisional dissipations (the last ones are represented by the term  $r_\mu$ ) occur.

It is possible to relate to each value of  $f(V)$ , computed through an empirical criterion, a couple of values  $r_\mu$ ,  $\phi_b$ , allowing to estimate the total run-out length obtained according to the empirical criterion. Referring to Corominas' criterion [8],  $\phi_b$  values are reported in **Table 2** for given  $r_\mu$ , angles  $\alpha$ , mobilized volume  $V$ .

The limit value  $r_\mu = 1$  gets conventional run-out lengths values according to the Mohr-Coulomb shear resistance law  $\phi_b(r_\mu = 1)$  at the base of the sliding mass.

If  $r_\mu > 1$ , energy dissipation, due to collisions localized in the basal shear layer [2,7,12], occurs.

To recover the run-out length estimated through the empirical law, it is necessary to assign a reduced friction angle, also depending by interstitial pressures at the base of the mass (not considered in the empirical criterion).

For high values of  $r_\mu$  (e.g.  $r_\mu = 3$ ), a friction angle allowing to estimate the same length forecasted by the empirical relationship cannot be determined.

Therefore, the mobilized friction angle  $\phi_b$ , smaller than the shear resistance angle  $\phi$  (static or almost static conditions), at the base of the mass, is conceptually admissible only if, contextually, collisional dissipations, due to granular temperature, are taken into account.

Values of  $\phi_b$ , for some  $r_\mu$  and  $\alpha$  values and dry ( $d/H = 1$ ) or saturated ( $d/H = 0$ ) conditions, are drawn in **Figure 5**.

**Table 2. Reduced shear resistance angle  $\phi_b$  values vs angle  $\alpha$ , for assigned  $r_\mu$  allowing to estimate the same run-out length obtained through the Corominas' relation  $f(V) = 10^{-0.85 \log V + 0.047}$ ;  $V = 10^6 \text{ m}^3$ ,  $\theta = 30^\circ$ ,  $L = 1000 \text{ m}$ ,  $l = 100 \text{ m}$ ,  $\gamma = 20 \text{ kN/m}^3$ ,  $\mu_\theta = 10^{-3} \text{ s}^2/\text{m}^2$ ,  $\lambda_\zeta = 0$ ,  $\chi_0 = 0.2$ .**

$\alpha [^\circ]$	$L_T [\text{m}]$	$r_\mu$	$\phi_b [^\circ]$	
			$d/H = 1$	$d/H = 0$
0	1645	1	19.2	37.5
		1.5	8	15.7
		3	6	11.8
-5	1516	1	19.4	38.2
		1.5	5.5	10.7
		3	2.6	5.4
-10	1433	1	19.7	38.7
		1.5	0.2	5.8
		3	—	—
-15	1375	1	19.8	39.5
		1.5	0.2	0.5
		3	—	—

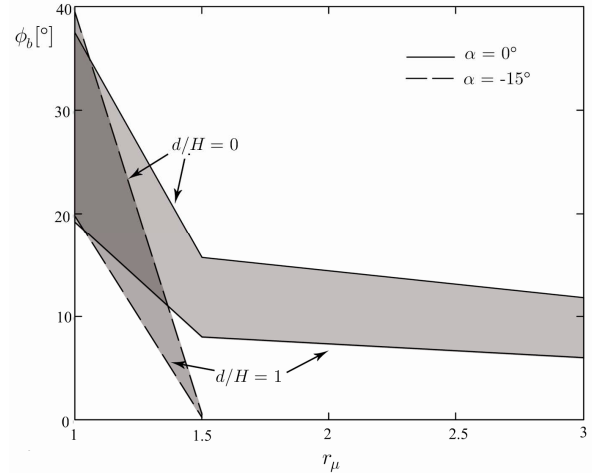


**Figure 5. Values of reduced shear resistance angle acting at the base of the block with the a-dimensional factor  $r_\mu$ .**

It is possible to highlight the existence of  $\phi_b$  ranges for different  $r_\mu$  values. It is worth observing that high counterslope values (e.g.  $\alpha = -15^\circ$ ) narrow the range of  $\phi_b(r_\mu)$ ; small  $r_\mu$  variations cause appreciable  $\phi_b$  variations.

## 5. Results

The run-out length, velocity and dissipated energy along the path, computed through the model ( $r_\mu = 1$ ,  $r_\mu = 1.1$  and  $r_\mu = 3.75$ ; further, for each case,  $\lambda_\theta = 0$ ,  $\lambda_\alpha = 0$ ,  $\chi_0 = 0.2$ ), are compared in **Figure 6** to the corresponding values obtained according to the Mohr-Coulomb (M-C) or Voellmy (V) resistance criterion at the base of the mass, neglecting the granular temperature effects.

The proposed model gets a run-out length equal to that one obtainable if the M-C resistance criterion is assumed at the base ( $r_\mu = 1$ ); conversely, by assuming  $r_\mu = 3.7$ , the computed run-out length is equal to the one estimated if the V criterion is applied at the base of the sliding mass. If  $r_\mu = 1.1$ , an intermediate run-out length is obtained.

For both cases, the sliding rate obtained through the model is smaller than the ones computed through M-C or V criteria; if  $r_\mu = 1$  the rate computed through the model is almost constant along an appreciable length of the path.

Computed rate and dissipated energy, for three  $\mu_\theta$  values, by assuming  $r_\mu = 1.5$ , are reported in **Figure 7**. The same values of the rate are compared with those ones obtained by assuming the M-C (three different friction angle) or V criterion (two values of turbulence coefficient  $\xi$ ) at the base of the mass. If the M-C-criterion is applied, high run-out distances (particularly for small  $\phi_b$ ), but excessive rate values, are obtained. Instead, if the V criterion acts, although obtained rate values are acceptable, small run-out lengths are obtained, because the hard

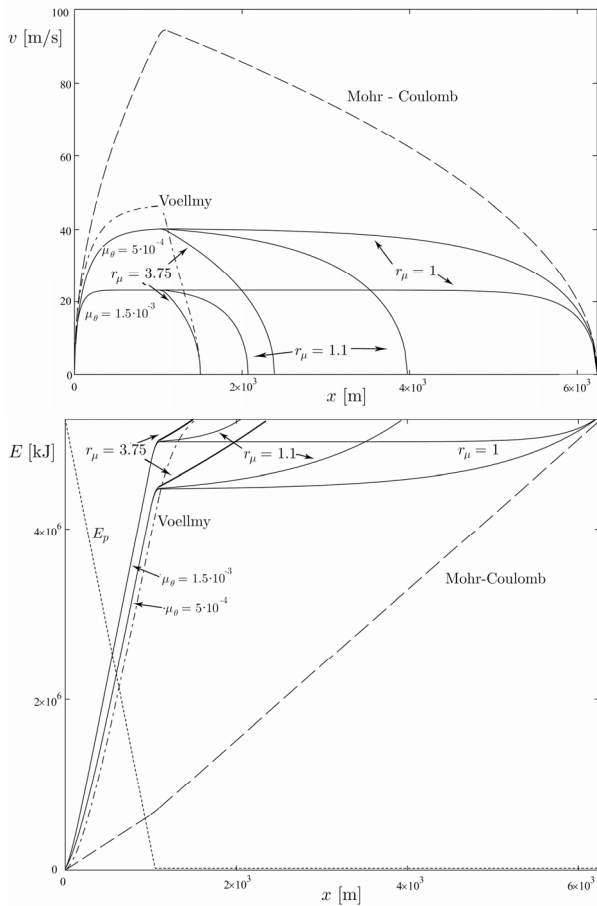


**Figure 6.** Velocity ( $v$ ) along the path and energy dissipation ( $E$ ) for three values of  $r_\mu$ ;  $L = 1000m$ ,  $l = 100 m$ ,  $H = 5 m$ ,  $d = 0 m$ ,  $\phi_b = 10^\circ$ ,  $\theta = 30^\circ$ ,  $\alpha = 0^\circ$ ,  $\gamma_t = 20 \text{ kN/m}^3$ . For Voellmy criterion,  $\xi = 1000 \text{ m/s}^2$ .

deceleration of the mass at the slope change. Computed run-out lengths  $L_T$  considerably vary with  $\alpha$  (counterslope, **Figure 8**) and ratio  $d/H$  (interstitial pressures at the base, **Figure 9**).

### 6. Back analysis

Only a partial assessment of the theoretical model [16,17] is possible, since direct field observations of landslides and avalanches are rarely available and are not directly applicable to estimate the above defined parameters. By taking into account these limits, the back analysis of the run-out length measured for the Frank slide (Canada, 1903) is carried out.

The Frank slide occurred on the morning April 29, 1903, killing about 70 people. The estimated mobilized volume was about  $30 \times 10^6 \text{ m}^3$ . The slope of the first sliding surface is about  $30^\circ$ , while for the counterslope is about  $-2.2^\circ$ . The profile along the run-out path is represented in **Figure 10**. A water saturated mass has been

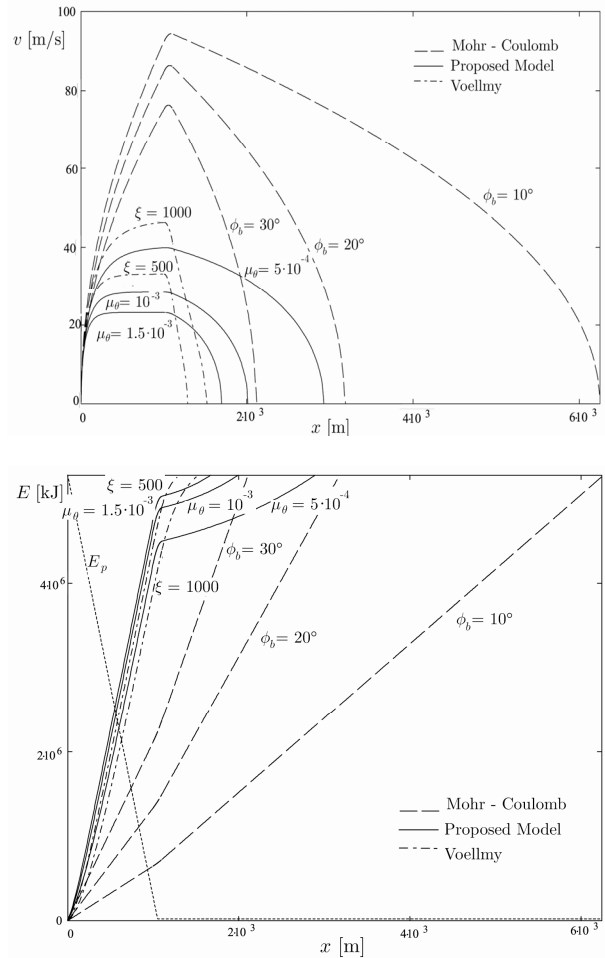


**Figure 7.** Velocity ( $v$ ) along the path and energy dissipation ( $E$ );  $L = 1000 m$ ,  $l = 100 m$ ,  $H = 5 m$ ,  $d = 0 m$ ,  $\theta = 30^\circ$ ,  $\alpha = 0^\circ$ ,  $\gamma_t = 20 \text{ kN/m}^3$ . For Voellmy criterion, it is assigned  $\phi_b = 10^\circ$ .

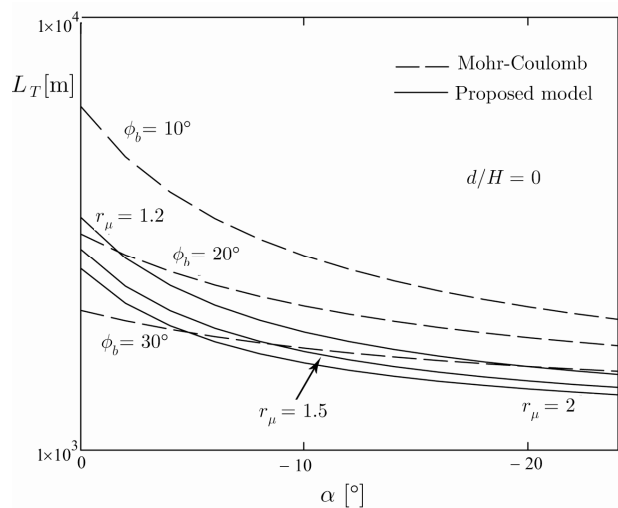


**Figure 8.** Total run-out length ( $L_T$ ) vs counterslope angle  $\alpha$ ;  $L = 1000 m$ ,  $l = 100 m$ ,  $H = 5 m$ ,  $\theta = 30^\circ$ ,  $\gamma_t = 20 \text{ kN/m}^3$ ,  $r_\mu = 1.5$ ,  $\lambda_\zeta \rightarrow 0$ ,  $\phi_b = 10^\circ$ ,  $\mu_\theta = 5 \cdot 10^{-4}$ .

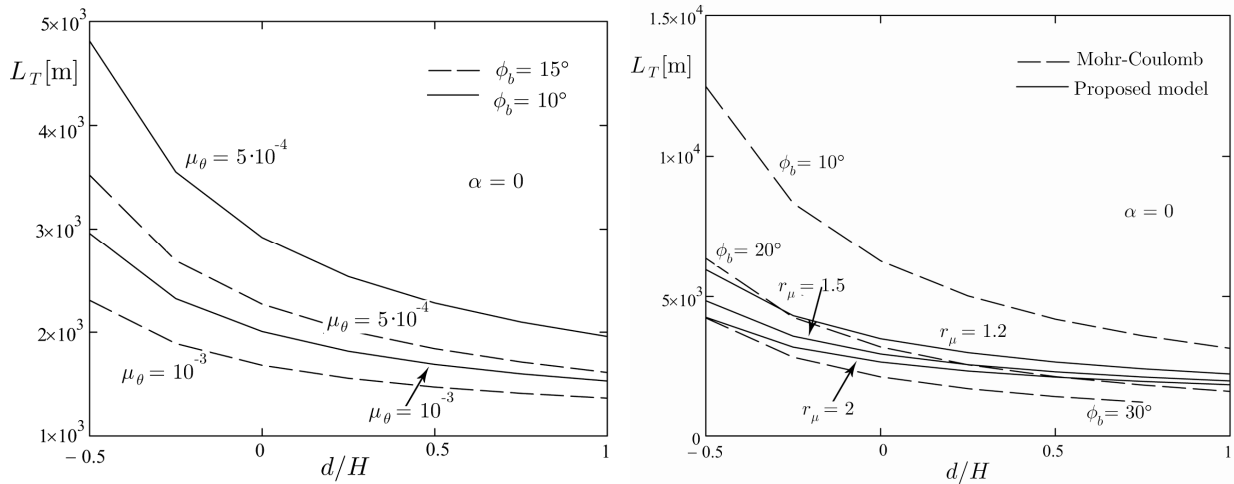


Figure 9. Total run-out length ( $L_T$ ) vs. ratio  $d/H$ ;  $L = 1000$  m,  $l = 100$  m,  $H = 5$  m,  $\theta = 30^\circ$ ,  $\gamma_l = 20$  kN/m<sup>3</sup>,  $r_\mu = 1.5$ ,  $\lambda_\zeta \rightarrow 0$ ,  $\phi_b = 10^\circ$ ,  $\alpha = 0^\circ$ ,  $\mu_\theta = 5 \cdot 10^{-4}$ .

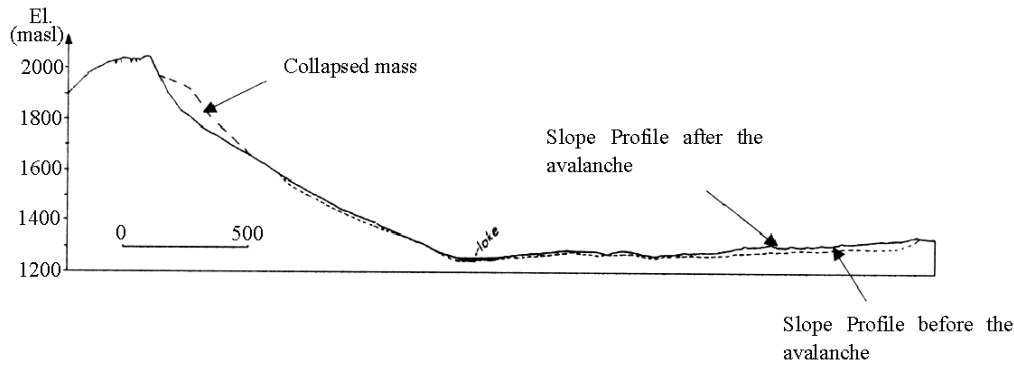


Figure 10. Frank slide: profile along the run-out path (modified from [17]).

assumed.

A basal shear resistance angle equal to  $16^\circ$  has been assigned, according to [16]. The parameters assigned to fit the measured run-out length  $L_T = 2800$  m are:  $\lambda_\theta = \lambda_\alpha = 5 \cdot 10^{-5}$  s/m,  $\chi_\theta = 0.1$ ,  $\mu_\theta = 3 \cdot 10^{-4}$  s<sup>2</sup>/m<sup>2</sup>.

The rate along the path is reported in **Figure 11**, for three  $r_\mu$  values. An acceptable agreement between measured and computed run-out lengths is achieved for  $r_\mu = 1.25$ .

The max rate of the sliding mass is 50 m/s, almost independently from the  $r_\mu$  values.

### 7. Concluding remarks

The motion of a granular mass along two planar s.s. is modeled accounting for granular temperature effects [6].

According to experimental observations and theoretical considerations, it is assumed that, during the rapid motion, a shear layer (s.l.) at the base of the sliding mass takes place [2,7,12]. Energy dissipation due to both frictional and collisional phenomena [13] and related storage

of kinetic energy, due to fluctuations of grains velocity, occur within this s.l.

The energy transferred by the s.l. (granular-inertial regime) to the sliding mass and *viceversa*, following a suggestion by [6], has been modeled by introducing a positive adimensional rate dependent function  $\chi_\zeta(v)$  in the power balance of the sliding mass.

By this way, the governing equations of the motion have been written with reference to the sliding along: 1) the first s.s.; 2) the progression from the first ( $\theta > 0$ ) to the second s.s. ( $\alpha < 0$ ); 3) the run-up along the second s.s. The assumption of a reduced shear resistance (mobilized angle  $\phi_b < \phi^*$ ) in Corominas' empirical criterion is conceptually justified *only if* the energy dissipation related to grains collisions, localized in the shear layer, is considered; a possible range of  $\phi_b$  values has been evaluated.

The "transfer" function  $\chi_\zeta(v)$  plays a role on the effects of energy dissipation and on the kinematic of the mass.

Moreover, along the first s.s., acceleration is smaller

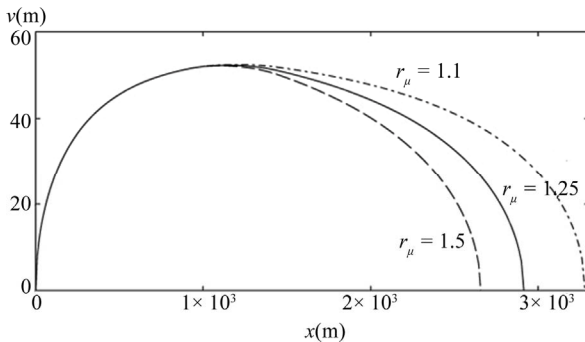


Figure 11. Frank Slide: rates along the run-out path.

than the one corresponding to a M-C shear resistance; along the second s.s., the deceleration assumes smaller values. Therefore, referring to the values computed through the M-C criterion (for the same value of angle  $\phi_b$ ), 1) the rate of the sliding mass at the end of the first s.s. is smaller; 2) run-up length along the second s.s will be greater (for the same rate at the beginning of the second s.s.) because the mass deceleration is smaller; 3) the total run-out length is always smaller, for  $r_\mu > 1$ .

To account for the different ways through which the energy is lost in collisions within the shear layer, along the two s.s., parameters  $\mu_\theta$ ,  $\mu_\alpha$  figuring in the  $\chi_s(v)$  function must be different ( $\mu_\theta \neq \mu_\alpha$ ).

Although neglected in empirical criteria, the slope  $\alpha$  of the second s.s. and the ratio  $d/H$  (G.W.T. conditions related to the mass depth) play a significant role.

The model allows to estimate considerable run-out lengths coupled with limited sliding rates, by this way overcoming some anomalies associated with the M-C or V-resistance criteria. For particular  $r_\mu$  values, the solutions obtained by assuming the M-C or Voellmy (V) resistance criteria are recovered.

The limits of the proposed model are mainly related to the invariability of the geometry of the sliding mass, the preliminary estimate of micromechanical parameters figuring in the laws motion, the uncoupling between the interstitial pressure at the base of the mass and the sliding rate.

## 8. Acknowledgments

This paper is dedicated to the memory of Prof. Antonino Musso, whose precious suggestions and remarks to the development of the proposed model are gratefully acknowledged.

## 9. References

[1] D. M. Cruden and D. J. Varnes, "Landslides Types and Processes," In A. K. Turner and R. L. Schuster Eds., *Landslides: Investigation and Mitigation*, National Acad-

emy Press, Washington, 1996, pp. 36-75.

- [2] S. Straub, "Predictability of Long Run-Out Landslide Motion: Implications from Granular Flows Mechanics," *Geologische Rundschau*, Vol. 86, No. 2, 1997, pp. 415-425. [doi:10.1007/s005310050150](https://doi.org/10.1007/s005310050150)
- [3] A. Musso, F. Federico and G. Troiano, "A Mechanism of Pore Pressure Accumulation in Rapidly Sliding Submerged Porous Blocks," *Computers and Geotechnics*, Vol. 31, No. 3, 2004, pp. 209-226. [doi:10.1016/j.compgeo.2004.02.001](https://doi.org/10.1016/j.compgeo.2004.02.001)
- [4] S. B. Savage and K. Hutter, "The Motion of a Finite Mass of Granular Material Down a Rough Inclined Plane," *Journal of Fluid Mechanics*, Vol. 199, 1989, pp. 177-215. [doi:10.1017/S0022112089000340](https://doi.org/10.1017/S0022112089000340)
- [5] K. T. Chau, "Onset of Natural Terrain Landslides Modelled by Linear Stability Analysis of Creeping Slopes with a Two-State Variable Friction Law," *International Journal for Numerical and Analytical Method in Geomechanics*, Vol. 23, No. 15, 1999, pp. 1835-1855. [doi:10.1002/\(SICI\)1096-9853\(19991225\)23:15<1835::AID-NAG2>3.0.CO;2-2](https://doi.org/10.1002/(SICI)1096-9853(19991225)23:15<1835::AID-NAG2>3.0.CO;2-2)
- [6] R. M. Iverson, M. E. Reid and R. G. Lahusen, "Debris-flow Mobilization from Landslides," *Journals of Earth and Planetary Sciences*, Vol. 25, 1997, pp. 85-138. [doi:10.1146/annurev.earth.25.1.85](https://doi.org/10.1146/annurev.earth.25.1.85)
- [7] D. Zhang and M. A. Foda, "An instability Mechanism for the Sliding Motion of Finite Depth of Bulk Granular Materials," *Acta Mechanica*, Vol. 121, No. 1-4, 1997, pp. 1-19. [doi:10.1007/BF01262520](https://doi.org/10.1007/BF01262520)
- [8] J. Corominas, "The Angle of Reach as Mobility Index for Small and Large Landslides," *Canadian Geotechnical Journal*, Vol. 33, No. 2, 1996, pp. 260-271. [doi:10.1139/t96-005](https://doi.org/10.1139/t96-005)
- [9] Y. S. Fang and Z. Y. Zhang, "Kinematic Mechanism of Catastrophic Landslides and Prediction of Their Velocities and Travelling Distance," *Landslides*, Lausanne, 1988.
- [10] D. Rickenmann, "Empirical Relationships for Debris Flows," *Natural Hazards*, Vol. 19, No. 1, 1999, pp. 47-77. [doi:10.1023/A:1008064220727](https://doi.org/10.1023/A:1008064220727)
- [11] A. E. Scheidegger, "On the Prediction of the Reach and Velocity of Catastrophic Landslides," *Rock Mechanics*, Vol. 5, No. 4, 1973, pp. 231-236. [doi:10.1007/BF01301796](https://doi.org/10.1007/BF01301796)
- [12] D. Zhang and M. A. Foda, "Internal Wave - Granular Temperature Interaction: An Energy Balance Study on Granular Flow," *Acta Mechanica*, Vol. 136, No. 3-4, 1999, pp. 155-170. [doi:10.1007/BF01179255](https://doi.org/10.1007/BF01179255)
- [13] N. Mitarai, H. Nakanishi, "Velocity Correlations in the Dense Granular Shear Flows: Effects on Energy Dissipation and Normal Stress," *Physical Review E*, Vol. 75, 2007.
- [14] R. A. Bagnold, "Experiments on a Gravity-Free Dispersion of Large Solid Spheres in a Newtonian Fluid under Shear," *Proceeding of the Royal Society*, Vol. 225, No. 1160, 1954, pp. 49-63. [doi:10.1098/rspa.1954.0186](https://doi.org/10.1098/rspa.1954.0186)
- [15] B. Salm, "Contribution to Avalanche Dynamics," in

*Proceeding of International Symposium on Scientific Aspects of Snow and Ices Avalanches*, Davos, 5-10 April 1965, pp. 199-214.

- [16] M. Pirulli and A. Mangeney, "Results of Back-Analysis of the Propagation of Rock Avalanches as a Function of Assumed Rheology," *Rock Mechanics and Rock Engineering*, Vol. 41, No. 1, 2008, pp. 59-84. [doi:10.1007/s00603-007-0143-x](https://doi.org/10.1007/s00603-007-0143-x)
- [17] A. Musso, F. Federico and M. Palmieri, "Proguex-A Code to Estimate the Run-Out Length of Granular Debris Flows," in Italian, in *Manuale di Ingegneria Civile ed Ambientale*, Vol. 1, 2003.
- [18] D. Ayotte, O. Hungr, "Assessment of Natural Terrain Landslide Debris Mobility," Geotechnical Engineering Office, Hong Kong, 1998.
- [19] H. Chen and C. F. Lee, "Numerical Simulation of Debris Flow," *Canadian Geotechnical Journal*, Vol. 37, No. 1, 2000, pp. 146-160. [doi:10.1139/t99-089](https://doi.org/10.1139/t99-089)
- [20] T. H. Erismann and G. Abele, "Dynamics of Rockslides and Rockfalls," Springer-Verlag, Berlin, 2001.
- [21] R. J. Fannin and T. P. Rollerson, "Debris flows: Some Physical Characteristics and Behaviour," *Canadian Geotechnical Journal*, Vol. 30, No. 1, 1993, pp. 71-81. [doi:10.1139/t93-007](https://doi.org/10.1139/t93-007)
- [22] A. Helmstetter, D. Sornette, J. R. Grasso, J. V. Andersen, S. Gluzman and V. Pisarenko, "Slider Block Friction Model for Landslides: Applications to Vaiont and La Clapière Landslides," *Journal of Geophysical Research*, Vol. 109, 2004. [doi:10.1029/2002JB002160](https://doi.org/10.1029/2002JB002160)
- [23] O. Hungr, "Model for the Run-Out Analysis of Rapid Flow Slides, Debris Flows, and Avalanches," *Canadian Geotechnical Journal*, Vol. 32, No. 4, 1995, pp. 610-623. [doi:10.1139/t95-063](https://doi.org/10.1139/t95-063)
- [24] O. Hungr and S. G. Evans, "Rock Avalanche Run out Prediction Using a Dynamic Model," *Proceeding of 7th International Symposium on Landslides*, Vol. 1, Trondheim, 1996, pp. 233-238.
- [25] H. J. Melosh, "The Mechanics of Large Rock Avalanches," *Reviews in Engineering Geology*, Vol. 7, 1987, pp. 41-49
- [26] M. Pirulli and G. Sorbino, "Effetto della Reologia sull'Analisi della Propagazione di Flussi di Detrito," Incontro Annuale dei Ricercatori di Geotecnica, Pisa, 2006.
- [27] P. Revellino, O. Hungr, F. Guadagno and S. G. Evans, "Velocity and Run-out Simulation of Destructive Debris Flows and Debris Avalanches in Pyroclastic Deposits Campania Region, Italy," *Environmental Geology*, Vol. 45, No. 3, 2003, pp. 295-311. [doi:10.1007/s00254-003-0885-z](https://doi.org/10.1007/s00254-003-0885-z)
- [28] S. B. Savage, "Flows of Granular Materials with Applications to Geophysical Problems," International Summer School on Mechanics, Udine, 1992.
- [29] M. Tiande, L. Zhougyu, N. Yonghang and M. Chongwu, "A Sliding Block Model for the Run-out Prediction of High-Speed Landslides," *Canadian Geotechnical Journal*, Vol. 38, No. 2, 2001, pp. 217-226. [doi:10.1139/t00-092](https://doi.org/10.1139/t00-092)
- [30] J. Vaunat, S. Leroueil, "Analysis of Post-Failure and Slope Movements within the Framework of Hazard and Risk Analysis," *Natural Hazards*, Vol. 26, No. 1, 2002, pp. 83-109. [doi:10.1023/A:1015224914845](https://doi.org/10.1023/A:1015224914845)